Supplemental Material for

"Spin fluctuations in $Sr_{1.8}La_{0.2}RuO_4$"

Zheng He, Qisi Wang, Yu Feng, Chul Kim, Wonshik Kyung, Changyoung Kim, Hongliang Wo, Gaofeng Ding, Yiqing Hao, Feiyang Liu, Helen C. Walker, Devashibhai T. Adroja, Astrid Schneidewind, Wenbin Wang, and Jun Zhao

X-ray diffraction on single crystals

We performed x-ray diffraction (XRD) measurements at room temperature on our $Sr_{1.8}La_{0.2}RuO_4$ single crystals used for the inelastic neutron scattering (INS) experiments at MERLIN and PANDA spectrometers. Fig. S1 displays a representative θ-2θ scan showing a series of the (0, 0, L) Bragg reflections with L = 2, 4, 6, 8, 10, 12, and 14. Rocking curve of the (006) reflection shows a sharp peak with the full-width-at-half-maximum (FWHM) fitted to be 0.10 degree. These results demonstrate the high quality of our $Sr_{1.8}La_{0.2}RuO_4$ single crystals.

Powder x-ray diffraction and the structure refinement

Powder XRD was performed on $Sr_{1.8}La_{0.2}RuO_4$ at room temperature (300 K) using a Bruker D8 Discover Diffractometer with a double crystal monochromator. Polycrystalline $Sr_{1.8}La_{0.2}RuO_4$ was obtained by grinding single crystals used in the inelastic neutron scattering experiments. The Rietveld analysis for the structure refinement was conducted using the FULLPROF software package. As shown in Fig. S2, all diffraction peaks can be indexed using one single phase with the same space group (I4/*mmm*) as undoped Sr_2RuO_4. No additional peaks, peak broadening, or diffuse scattering are observed, revealing no detectable impurity or disorder. The refinement results, summarized in Table S1, show that the actual concentrations of Sr and La are 1.827 ± 0.065 and 0.173 ± 0.065, respectively, which agree with the nominal values within the error range.

Electron-probe microanalysis experiments

Electron-probe microanalysis (EPMA) was performed to determine the chemical concentrations. Two pieces of single crystal (#1 and #2) used for the INS experiments were measured. Five different positions were analyzed for each sample and the results are summarized in Table S2. For sample #1, the average Sr and La concentrations are 1.816 ± 0.101 and 0.226 ± 0.033, respectively. For sample #2, the average Sr and La concentrations are 1.809 ± 0.042 and 0.197 ± 0.023, respectively. Both Sr and La chemical concentrations determined by the EMPA are very close to their nominal values, consistent with the XRD refinement results.

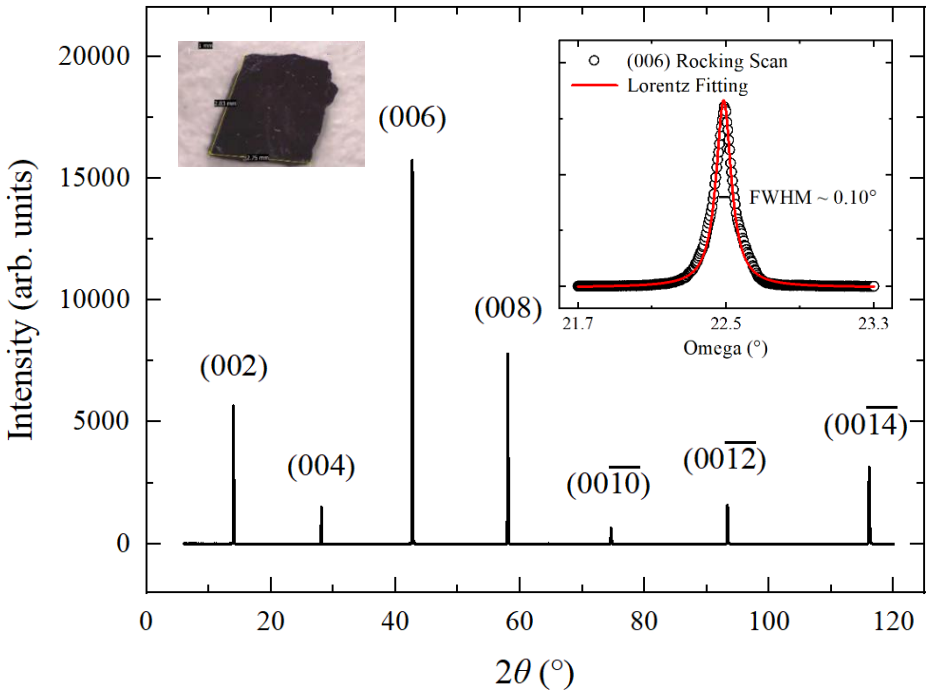

Fig. S1. XRD patterns of a $Sr_{1.8}La_{0.2}RuO_4$ single crystal measured at room temperature with the x-ray wavelength λ = 1.5406 Å. The left inset shows the photograph of the measured single crystal, and the right inset displays the rocking scan of the (006) Bragg peak fitted with a Lorentzian profile (red solid curve).

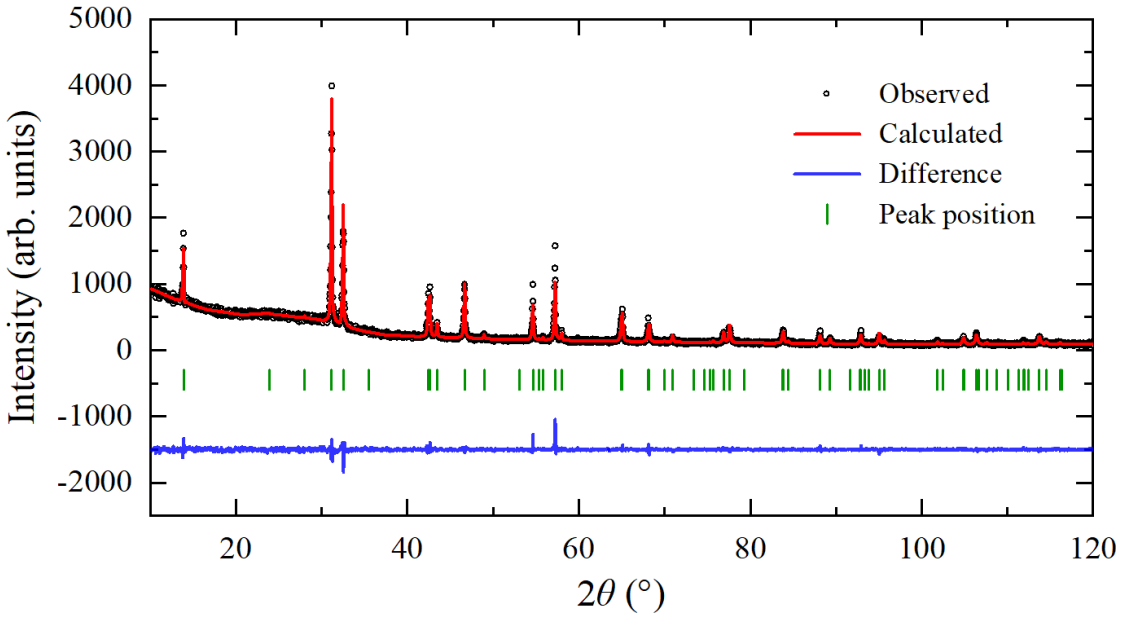

Fig. S2. Powder XRD pattern of $Sr_{1.8}La_{0.2}RuO_4$ measured at room temperature with the x-ray wavelength λ = 1.5406 Å. Open circles are experimental data and green vertical bars indicate the positions of Bragg reflections. The red curve shows a calculated diffraction pattern, and the blue curve is the difference between experimental and calculated intensities.

Table S1. Refined crystallographic parameters of $Sr_{1.8}La_{0.2}RuO_4$ (T = 300 K)

Space group: I4/*mmm* with $a = b$ = 3.88536(11) & c = 12.70594(36) Å R_{wp} (%) = 7.36, R_p (%) = 5.43, χ^2 = 1.38						
Atom	Position	x	y	z	B(Å^2)	Occupancy
Sr	4*e* 4*mm*	0	0	0.35384(21)	0.348(105)	1.827(65)
La	4*e* 4*mm*	0	0	0.35384(21)	0.348(105)	0.173(65)
Ru	2*a* 4/*mmm*	0	0	0	0.339(127)	1
O(1)	4*c mmm*	0	0.5	0	0.307(469)	2
O(2)	4*e* 4*mm*	0	0	0.16535(177)	2.205(441)	2

Table S2. Summary of EPMA results on $Sr_{1.8}La_{0.2}RuO_4$

		Mole Percentage (%)			Mole Ratio (Normalized to Ru)		
Sample No.	Position	Sr	La	Ru	Sr	La	Ru
Sample #1	A	24.294	4.208	14.953	1.625	0.281	1.000
	B	26.997	3.242	14.564	1.854	0.223	1.000
	C	26.560	3.378	14.517	1.830	0.233	1.000
	D	26.958	3.164	14.613	1.845	0.217	1.000
	E	27.953	2.595	14.502	1.928	0.179	1.000
	Average	26.552	3.317	14.630	**1.816**	**0.226**	1.000
	Std. Error	1.219	0.519	0.166	**0.101**	**0.033**	0
Sample #2	F	27.135	3.230	14.488	1.873	0.223	1.000
	G	25.909	2.910	14.716	1.761	0.198	1.000
	H	25.707	3.211	14.545	1.767	0.221	1.000
	I	26.383	2.404	14.353	1.838	0.167	1.000
	J	26.686	2.604	14.771	1.807	0.176	1.000
	Average	26.364	2.872	14.575	**1.809**	**0.197**	1.000
	Std. Error	0.517	0.327	0.152	**0.042**	**0.023**	0

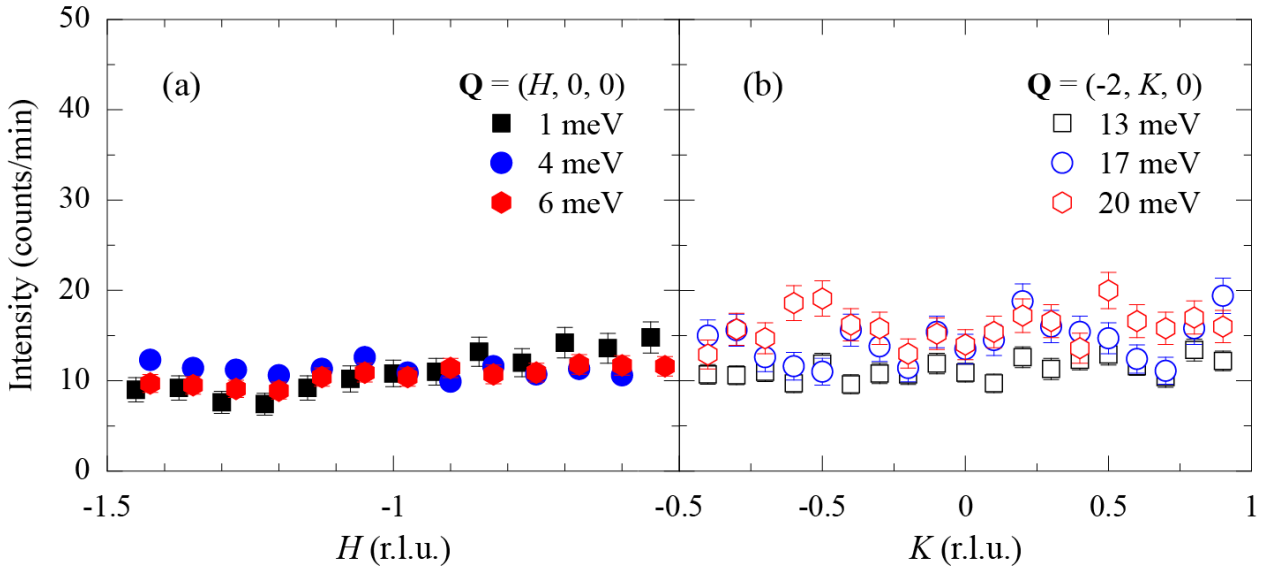

Fig. S3. Constant-energy scans measured on cold neutron three axes spectrometer PANDA with the final neutron energy of E_f = 5.1 meV at 4 K. (a) Constant-energy scans along the H direction through (-1, 0, 0) with energy transfer of E = 1 (filled squares), 4 (filled circles) and 6 (filled hexagons) meV. (b) Constant-energy scans along the K direction through (-2, 0, 0) with energy transfer of E = 13 (open squares), 17 (open circles) and 20 (open hexagons) meV.

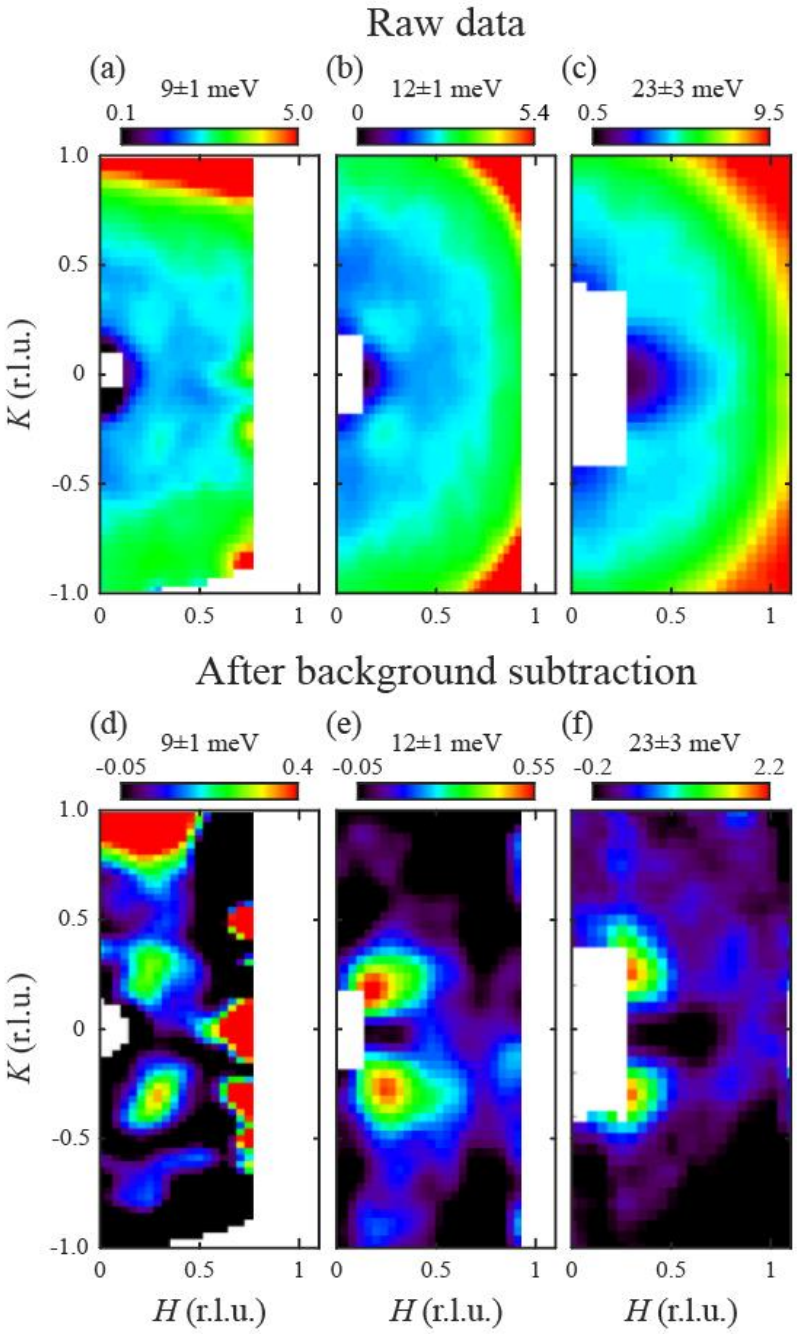

Fig. S4. Representative raw data in the *H*-*K* plane with incident neutron energies of E_i=18.8 (a), 40.2 (b) and 135.8 meV (c), and the corresponding constant-energy images after background subtraction (d-f), following the method described in Ref. [1].

Reference:

[1] Q. Wang, Y. Shen, B. Pan, X. Zhang, K. Ikeuchi, K. Iida, A. D. Christianson, H. C. Walker, D. T. Adroja, M. Abdel-Hafiez, X. Chen, D. A. Chareev, A. N. Vasiliev, and Jun Zhao, Magnetic ground state of FeSe, Nat. Commun. **7,** 12182 (2016).